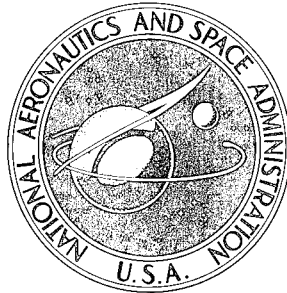


NASA TECHNICAL NOTE



NASA TN D-8006

NASA TN D-8006

FRICITION AND WEAR OF  
CARBON-GRAPHITE MATERIALS  
FOR HIGH-ENERGY BRAKES

*Robert C. Bill*

*Lewis Research Center*

*and U.S. Army Air Mobility R&D Laboratory*

*Cleveland, Ohio 44135*

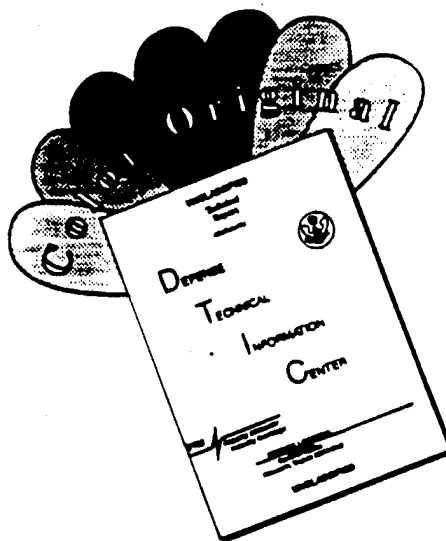
19960424 056

MASTER

022385



# DISCLAIMER NOTICE



THIS DOCUMENT IS BEST QUALITY AVAILABLE. THE COPY FURNISHED TO DTIC CONTAINED A SIGNIFICANT NUMBER OF COLOR PAGES WHICH DO NOT REPRODUCE LEGIBLY ON BLACK AND WHITE MICROFICHE.

1. Report No. NASA TN D-8006	2. Government Accession No.	3. Recipient's Catalog No.	
4. Title and Subtitle FRICION AND WEAR OF CARBON-GRAPHITE MATERIALS FOR HIGH-ENERGY BRAKES		5. Report Date June 1975	6. Performing Organization Code
		8. Performing Organization Report No. E-8259	10. Work Unit No. 505-04
7. Author(s) Robert C. Bill		11. Contract or Grant No.	
9. Performing Organization Name and Address NASA Lewis Research Center and U.S. Army Air Mobility R&D Laboratory Cleveland, Ohio 44135		13. Type of Report and Period Covered Technical Note	
		14. Sponsoring Agency Code	
12. Sponsoring Agency Name and Address National Aeronautics and Space Administration Washington, D. C. 20546		15. Supplementary Notes	
16. Abstract Caliper-type brake simulation experiments were conducted on seven different carbon-graphite material formulations against a steel disk material and against a carbon-graphite disk material. The effects of binder level, boron carbide (B <sub>4</sub> C) additions, graphite fiber additions, and graphite cloth reinforcement on friction and wear behavior were investigated. Reductions in binder level and additions of B <sub>4</sub> C each resulted in increased wear. The wear rate was not affected by the addition of graphite fibers. Transition to severe wear and high friction was observed in the case of graphite-cloth-reinforced carbon sliding against a disk of similar composition. This transition was related to the disruption of a continuous graphite shear film that must form on the sliding surfaces if low wear is to occur. The exposure of the fiber structure of the cloth constituent is believed to play a role in the shear film disruption.			
17. Key Words (Suggested by Author(s)) Friction; Wear; Graphite; Carbon; Brakes; Surface layers; Oxidation		18. Distribution Statement Unclassified - unlimited STAR category 27 (rev.)	
19. Security Classif. (of this report) Unclassified	20. Security Classif. (of this page) Unclassified	21. No. of Pages 28	22. Price* \$3.75

\* For sale by the National Technical Information Service, Springfield, Virginia 22151

# FRICITION AND WEAR OF CARBON-GRAPHITE MATERIALS FOR HIGH-ENERGY BRAKES

by Robert C. Bill

Lewis Research Center and  
U. S. Army Air Mobility R&D Laboratory

## SUMMARY

Seven different carbon-graphite material formulations were evaluated in caliper-type brake simulation experiments. The carbon-graphite pad materials were subjected to sliding against a 17-22 AS steel disk material and against a graphite-cloth-reinforced composite disk material. Typical sliding speeds and normal loads were 31 m/sec (100 ft/sec) and 382 N (86 lbf), respectively. Frictional behavior and wear rates based on weight loss measurements were used, in conjunction with microscopic examination of the sliding surface, to evaluate material performance and to identify wear mechanisms. It was observed that increased wear accompanied both reductions in the binder level and additions of boron carbide ( $B_4C$ ) to the basic carbon-graphite material formulation. A friction and wear instability was identified in the case of graphite-cloth-reinforced carbon sliding against a disk of similar composition and structure. Heavy wear to the disk and irregular, high friction were observed after an initial period of low wear and smooth friction. This transition was observed to be irreversible in that once it occurred it continued through subsequent sliding contact exposures. The severe wear and high friction seemed to be related to the disruption of and inability to reform a continuous, preferentially oriented graphite shear film on the sliding surfaces. The exposure of the continuous fiber structure of the cloth constituent at the sliding surface is believed to play a role in the shear film disruption.

## INTRODUCTION

High friction forces resulting from heavy unit loads and high sliding velocities produce large quantities of energy in such mechanical components as clutches, brakes, sliding-element bearings, and under certain conditions, seals. In terms of rate of

energy dissipation, the most severe situation is probably to be found in aircraft brake systems. Here typical brake applications require the sliding interfaces to convert about  $4200 \text{ N}\cdot\text{m}/\text{cm}^2$  ( $20\,000 \text{ ft}\cdot\text{lb}/\text{in.}^2$ ) of kinetic energy per unit area to heat in approximately 30 seconds (ref. 1). Unless improved materials for brake linings are developed, the trend toward heavier aircraft will result in either shorter brake lining lives, which will increase maintenance, or larger brake lining area, which will increase landing gear weight and bulk.

The life of currently used aircraft brake lining materials is determined by wear, which in turn is strongly dependent on the temperature experienced by these materials during sliding. This temperature dependence is due largely to softening of the metal binder (usually copper or iron) present in the currently used brake lining composite materials (ref. 2). In addition, the thermal cycling promotes cracking and spallation, which results in accelerated wear (ref. 3) and oxidation.

In view of the problems associated with metal-based composites, two properties that a superior material for use as an aircraft brake lining should possess become apparent. These properties are (1) significant mechanical strength at temperatures approaching  $1100^\circ \text{C}$  ( $2012^\circ \text{F}$ ) and (2) a low thermal expansion coefficient to reduce thermal stresses caused by temperature gradients. Improvements in these two properties would result in reduced wear, provided they are not accompanied by reduced thermal conductivity, reduced volume specific heat, or tendencies to undergo adhesive wear.

There are several material approaches that might be considered from the standpoint of these requirements. Among them are the use of ceramics rather than metal-based composites and the substitution of higher temperature metals for the currently used copper (refs. 4 and 5). The approach considered herein is to construct part or all of the brake system (lining and heat-sink material) of carbon graphite. Carbon-graphite materials have demonstrated good friction and wear properties in that they are nongalling and tend to be self-lubricating (ref. 6). Their attractive thermal properties include a conductivity comparable to that of metals, a very high mass specific heat, and almost a 100-percent retention of mechanical properties at temperatures to  $1100^\circ \text{C}$ . However, like the ceramic materials, the carbon graphites do tend to be brittle. Another potential problem with carbon-graphite materials is their susceptibility to oxidation (ref. 7). Limited military experience with carbon-graphite brake materials indicates that the oxidation problem is not so severe as was initially suspected. At the sliding interface, the location of maximum temperature, exclusion of air effectively inhibits oxidation.

This work was conducted to determine the friction and wear behavior of a series of carbon-graphite materials in a high-energy friction situation, similar to that encountered in brake applications. The materials selected for this study are intended to show the effects of concentration of carbon binder, changes in filler constituents, additions of an oxidation inhibitor, and the presence of a graphite cloth reinforcement on high-energy friction and wear.

The investigation was performed on a caliper-type brake simulation apparatus. Sliding speeds to 31 m/sec (100 ft/sec) were used with typical normal unit loads of 88 N/cm<sup>2</sup> (127 psi). Wear rates were based on weight loss measurements after sliding. Friction was continuously recorded for all experiments. Optical and scanning electron microscopy (SEM) were used to help identify the wear mechanisms.

## APPARATUS

The apparatus used in this study is shown in figure 1. It consisted of a 35.6-cm- (14-in.-) diameter brake disk driven by a 30-kW (40-hp) electric motor. The carbon-graphite pad specimens were loaded, caliper fashion, against the disk by a pair of hydraulic cylinders. Both specimens were fully loaded against the disk within less than 1/2 second of one another. The grip assembly contained a ball-in-socket mounting to provide for specimen alignment with respect to the disk. The support holding the specimens and hydraulic cylinders was suspended from the stationary framework by a pair of flexible plate assemblies, which allowed for the transmission of the friction force to a strain-gage ring mounted on the framework. The rotational speed and normal force between the specimen and the disk were also measured.

The experimental carbon-graphite pads were 2.54 cm (1 in.) in diameter with a 0.95-cm- (3/8-in.-) diameter hole in the center for mounting purposes. An antirotation slot was provided on the back of each pad, as was a thermocouple hole that allowed for temperature readings at a depth of 1 to 1.5 mm (0.04 to 0.06 in.) below the sliding surface of the pad.

Frictional force, normal load (hydraulic pressure), disk speed, and the temperature indicated by the thermocouples in each pad were constantly recorded. These measured data were supplemented by observations concerning noise level during sliding, occurrence of sparking or burning of pad material, and generation of loose debris.

## MATERIALS

The properties and compositions of the experimental carbon-graphite pad materials are shown in table I. With the exceptions of graphite-cloth-reinforced composite (GCRC) and boronated graphite (BG), the processing of these carbon-graphite materials was similar (ref. 8) and is briefly summarized here. The filler and binder constituents were mixed in the indicated proportions, and the mixture was molded under the indicated temperature and pressure conditions. The compacts were then heat treated according to a carefully controlled heating and cooling schedule during which a maximum tempera-

ture of 2800° C (5072° F) was reached and held for 1 hour. During the heating cycle, volatile substances from the binder were driven off, leaving behind a completely carbonized binder phase. At the extreme temperatures, some graphitization of the binder also occurred.

The GCRC material was prepared by binding layers of woven graphite cloth together, the binder being a pitch material. The composite was then subjected to a high-temperature heat treatment during which the binder between the cloth plies was carbonized.

The BG material is a highly graphitic matrix material with the addition of approximately 10 percent (by weight) of boron carbide ( $B_4C$ ). The binder used was coal tar pitch, a material that extensively graphitizes during the 2800° C treatment. The exact proportion of pitch binder is unknown but is believed to be about 30 parts by weight per 100 parts of graphitic filler material.

Two disk materials were used: 17-22 AS steel (currently used aircraft brake disk material) and a graphite-cloth-reinforced carbon material (similar to the GCRC pad material). The nominal composition of the 17-22 AS steel was Fe-0.3C-1.3Cr-0.5Mo-0.25V. It was heat treated to a hardness of 45 Rockwell C.

## PROCEDURE

The experimental carbon-graphite pad specimens were dry machined to a 0.4- $\mu$ m (10- $\mu$ in.) surface finish, lightly sanded on dry 600-grit polishing paper, and then burnished against a lint-free cloth. They were next baked at 200° C (392° F) for 2 hours in an effort to drive off residual contaminants. Following this treatment they were stored in a desiccator until removed for testing.

The 17-22 AS steel disks were ground to a 0.4- $\mu$ m surface finish and cleaned with trichloroethylene before use in a test. A fresh steel disk was used for each pair of carbon-graphite pad specimens. The graphite-cloth-composite disks were used in the as-received condition, and no solvent treatments were applied before testing. Because of the limited number of graphite-cloth-reinforced composite disks available, it was necessary to run more than one test with each disk.

The wear calculations were based on pretest and post-test weight measurements of the pad specimens. Since typical weight losses were of the order of several milligrams, there was concern about the effect of moisture absorption on the weight measurements. It was found that, within 1 hour after bake-out, the pad weight stabilized; further exposure to laboratory environment for several days resulted in weight fluctuations of 1 mg ( $2 \times 10^{-6}$  mlb) or less. Thus, 1 hour after removal from the desiccator, the pre-test weight measurements were made. Similarly, the post-test weight measurements were made approximately 1 hour after a sliding exposure.

After the pretest weight measurements, the specimens were fastened into the holders, thermocouples were inserted in a hole in the back of each pad, and the pads were loaded against the stationary disk surface. The ball-in-socket joints were tightened, and the pads were unloaded. The specimens were thus aligned with respect to the disk surface.

Three types of brake tests were conducted in this investigation. The first type was designed to indicate the frictional behavior of the pad materials under conditions of varied sliding speed. The test pattern consisted of three simulated-stop applications followed by three constant-speed applications, followed by a final simulated stop. The simulated stop was conducted by driving the disk at 1800 rpm, which gave a 31-m/sec surface speed. The motor power was then switched off and the brake pads were loaded against the disk with a 765-N (172-lbf) force, braking the disk and motor rotor to a stop. The constant-speed applications were performed by loading the pads with a 765-N normal force against the disk for 10 seconds, with the disk driven at constant speed. The three constant-speed applications were at 31, 26, and 20 m/sec (100, 83, and 67 ft/sec). The pads were visually inspected (in the holders) after the first three simulated-stop exposures to determine whether they were damaged or excessively worn before they were subjected to the more severe constant-speed exposures.

The second test pattern was a load-variation test consisting of sequentially loading the pads under incrementally increased normal loads while the disk was rotated at a constant 26 m/sec. The normal loads were 186, 227, 302, 382, 422, 462, 502, and 542 N (42, 51, 68, 86, 95, 104, 113, and 120 lbf) and the contact time was 10 seconds.

Finally, the third type of test was conducted by subjecting the experimental pad materials to a 422-N normal load and a 26-m/sec sliding velocity for an uninterrupted exposure of 60 seconds. The motivation for this type of test was to determine whether frictional transitions and changes in wear mechanisms might accompany prolonged sliding exposures.

The measured weight losses were translated into wear volumes. The wear volumes were then divided by the frictional energy dissipated during sliding to give a specific wear rate which would reflect both the wear of the pad material and its performance as a brake. The pad sliding surfaces were then photographed, and in some cases, scanning electron microscopy observations of the sliding surface features were made.

## RESULTS AND DISCUSSION

### General Frictional Behavior

The carbon-graphite - high-binder (CG-HB) material served as a standard for the comparison of the friction and wear behavior of the different carbon-graphite formula-

tions. Figures 2(a) and (b) show friction data obtained when CG-HB was subjected to sliding against the 17-22 AS steel disk material. With some exceptions, to be noted later, these results are typical of the friction behavior exhibited by most of the carbon-graphite materials during sliding against both the 17-22 AS steel and graphite-cloth-reinforced disk materials. The friction was very smooth and uniform (friction coefficient,  $\mu \approx 0.22$ ) during the constant-speed exposures. A slight increase in friction (to  $\mu \approx 0.27$ ) was observed toward the end of the stop. Notice that most of the friction increase took place after the sliding speed had been reduced to about 16 m/sec (52 ft/sec), as shown in figure 2(b).

When the carbon-graphite materials were subjected to sliding in a load-variation test configuration, somewhat lower values of friction were measured, as indicated in the summary of friction-against-load results shown in table II(a). Furthermore, the variation of friction coefficient with normal load was irregular, with the values of friction coefficient usually being higher under high normal loads than under low normal loads. Comparing tables II(a) and (b) shows that all carbon-graphite materials, with the exception of GCRC, experienced higher friction when sliding against the graphite-cloth-reinforced disk than against the 17-22 AS steel disk material.

Under prolonged, high-normal-load sliding conditions against 17-22 AS steel disks, the carbon-graphite materials usually underwent a transition to high, rough friction. The results shown in figure 3 are typical. The load in this case was 463 N (104 lbf). After about 20 seconds of sliding, considerable vibration began to appear in the frictional force measurement. After 30 seconds the friction was clearly rising and an audible squeal accompanied the much larger vibration. At the end of the exposure, after 35 seconds of sliding, the coefficient of friction was about 0.25, compared to 0.16 at the beginning. Details as to the magnitude of such transitions and the time required for them to occur varied from test to test and did not seem to be a function of the carbon-graphite pad material formulation. In some cases these transitions were seen to be reversible - the friction returning to a value close to that initially observed and again becoming smooth. In other cases the friction became so high and the vibration so severe that fracture of the pad material occurred.

The wear results summarized in table III indicate that some of the carbon-graphite materials exhibited exceptionally severe wear when sliding against 17-22 AS steel in either a load-variation or a prolonged-exposure test, but never in a simulated-stop - speed-variation test. The generation of sparks, which is indicative of oxidation at the interface, was observed to accompany the severe wear. The sparks, and probably most of the wear, occurred during the heavy load applications of the load-variation tests and near the end of the 60-second applications when bulk pad temperatures of 150° to 200° C (302° to 392° F) were measured. The weight change incurred during these exposures was usually much higher than that resulting from tests in which sparking was not ob-

served, and the bulk of the specimen weight loss most likely resulted from oxidation rather than sliding wear. These results were not included in the calculation of average wear rates, but their occurrence is significant in assessing the performance of the experimental carbon-graphite materials.

### Surface Shear Layer Observations

Studies of the surface characteristics of the carbon-graphite pads indicate that during sliding the shear takes place in a thin reoriented layer that forms on the pad surface. This concept is discussed in references 6 and 9. Figure 4 shows the surface condition of a CG-HB specimen after a combination of simulated-stop and speed-variation exposures against a 17-22 AS steel disk. This surface is typical of all the carbon-graphite sliding surfaces after such sliding exposures. In these cases, transfer films were also seen on the disk surface. Very few features were apparent in the reoriented layer that developed on the carbon-graphite pad sliding surface. When viewed in room light the layer exhibited a mirrorlike polish.

After exposure to conditions that produced the type of transition described in figure 3, the sliding surface of the carbon-graphite pads showed a distinctly different appearance. On a microscopic scale the sliding surface of the pads showed elongated "blisterlike" features that had a metallic appearance in room light. These features covered about 10 to 20 percent of the surface, the remainder having an appearance like that in figure 4. Examples of these "blistered" areas are shown in figure 5. Here the "blistered" areas are seen to be regions where the shear layer is disrupted; some structural detail is revealed by the way in which the layer breaks up. The shear layer is seen to consist of distinct sheets, probably composed of preferentially oriented graphite. Regions of graphite sheet that have buckled and fractured, with resulting separation from the substrate, are revealed by the "glowing" white areas. The transition to higher friction may then be related to the disruption of a dense, continuous surface shear layer composed of oriented sheets of graphite. According to the literature, disruption can be induced (1) by the desorption of water and other vapors from the shear layer (refs. 6 and 10) and/or (2) by the disruption of the surface oxide present on the metal disk (ref. 9). Once the shear layer is broken up, the pad sliding surface is composed of randomly oriented carbon and graphite particles. Unless the shear layer is restored, sliding will continue to be in a high friction and wear mode.

Figure 6 shows the surface of a carbon-graphite pad after very severe sliding ( $\mu > 0.5$ ) with heavy wear. No coherent film exists, and there are pockets of loose debris particles at various locations on the surface. On a macroscopic scale the sliding surface of the pad exhibits a matte appearance, typical of the surface of carbon-

graphite materials after undergoing oxidation. The frictional heating was such that pad temperatures of 150<sup>o</sup> to 200<sup>o</sup> C were measured at a 1-mm depth below the sliding surface. Simple heat-transfer considerations indicate that the temperature could easily exceed 600<sup>o</sup> C (1112<sup>o</sup> F) at the sliding surface, which would promote oxidation of the surface regions.

### Comparison of Wear Results

Effect of binder level. - Wear results for the seven experimental pad materials are shown in tables III(a) and (b) for sliding against 17-22 AS steel and graphite-cloth-reinforced composite disks, respectively. It is apparent that the relative pad material performance depends on the composition of the disk material.

The effect on wear of varying the amount of pitch binder in the prebake mix may be seen by comparing the performance of CG-HB, CG-MB, and CG-LB (carbon graphite with high, medium, and low binder levels, respectively). For sliding against both the 17-22 AS steel and graphite-cloth-reinforced composite disks, the medium-binder-level material (60 parts by weight per 100 parts filler) CG-MB showed a significantly higher wear rate than either the high- or low-binder-level materials (CG-HB and CG-LB).

There are three factors that might account for the observed wear trend. First, the graphite shear film formation properties of the carbon graphite might be adversely affected by increasing the binder level (thus decreasing the overall graphite content). Second, the higher-binder-level carbons are more prone to oxidation because of the less graphitic structure and the greater porosity associated with the binder constituent. (No sparking was observed during the tests on CG-LB.) These two factors explain the increased wear rate of CG-MB compared to CG-LB. The third factor associated with the binder level is a general improvement in mechanical properties that accompanies an increase in concentration of the binder constituent, as is shown in table I(b). This factor is probably responsible for the reduced wear rate of CG-HB compared to CG-MB.

Effect of chopped carbon fiber additions. - The addition of finely chopped carbon fibers to the filler (in place of the nongraphitic component) of the high-binder-level formulation (CG-FF) resulted in some reduction in wear rate during sliding against both disk materials. This may be seen in table III by comparing CG-FF with CG-HB.

A pattern of increasing friction with time of application was observed when CG-FF was subjected to sliding against 17-22 AS steel. A typical case is shown in figure 7. None of the other carbon graphites exhibited this phenomenon. Also, as shown in table II, the highest friction against the graphite-cloth-reinforced composite disk was observed in the case of CG-FF.

An SEM study was made of the features present on the surface of a CG-FF pad which had been subjected to sliding against a 17-22 AS steel disk. Fiber segments were visible on the wear surface shown in figure 8, and there were signs of interaction of the fibers with the film formed on the pad surface. In particular, surface striations can be seen in figures 8(a) and (b), which suggests an abrasive interaction between the fiber segments and the sliding surfaces. The interaction would have to be caused by loose, broken pieces of fibers as they moved out of the contact area. The fibers constitute comparatively hard, discrete bodies on the sliding surface and have sharp corners and edges generated by fracture. Loose, broken fiber segments certainly have the potential to mechanically disrupt the softer low-shear-strength film - much as an abrasive would. It is a question of fiber concentration as to whether this effect will result in a higher macroscopic wear rate.

Effect of  $B_4C$  additions. - Boron carbide is added to mechanical carbons in order to improve their high-temperature oxidation resistance (refs. 7 and 8). Table III(a) shows that the carbon graphite with  $B_4C$  additions (CG-BC) underwent a higher wear rate than the basic formulation (CG-HB) when sliding against the 17-22 AS steel disk material. The higher wear rate was most likely the result of abrasive action by particles of  $B_4C$  additive. However, when considering a full-scale brake application, a trade-off must be made between material loss due to higher wear at the sliding surfaces and loss of properties due to oxidation. An increase in the former may be more than compensated for through improved oxidation resistance afforded by the  $B_4C$  additions. Indeed, no instances of spark generation with its associated heavy oxidation wear were observed with CG-BC. Firm conclusions regarding the benefits to be obtained through  $B_4C$  additions to high-energy-brake carbon formulations require full-scale experience.

Friction and wear of graphite-cloth-reinforced composite. - The graphite-cloth-reinforced composite (GCRC) pads were the most wear resistant of the experimental carbon materials when sliding against the 17-22 AS steel disk material. After a sliding exposure, the pad sliding surfaces had a polished appearance with the structure of the graphite cloth apparent, as shown in figure 9. The continuous fiber structure of the composite had remained essentially intact with a continuous film smeared over the sliding surface. Figure 9(b), an SEM photograph, shows the fiber structure barely visible through the surface film.

The friction and wear of GCRC pads in sliding contact with the graphite-cloth-reinforced disk were markedly different from the preceding results. Even though wear rates to the pads (table III(b)) were not significantly higher, instances of unstable transitions to severe wear and high, irregular friction (not reflected in the values shown in table II) were observed. Furthermore, these transitions seemed to be irreversible. That is, once they occurred, severe wear and high friction were observed on subsequent sliding exposures, even after sufficient time intervals to allow for specimen cooling, as

shown in figure 10. The severe wear was accompanied by the generation of clouds of loose carbon debris being spewed from the contact area. The condition of the GCRC pad surface after such a sliding exposure was significantly different from that shown in figure 9. Exposed fibers are obvious in the SEM photographs of figure 11. A remarkable feature of the GCRC material shown in these photographs is the very irregular, sharp-edged fiber cross section. The lack of any coherent shear layer on the pad sliding surface is good evidence that fiber exposure ultimately leads to the disruption of this layer. The shape of the fibers and the high mechanical strength associated with them would enable them to act as potentially abrasive constituents on the pad surface.

The surface condition of the graphite-cloth-reinforced disk was similar to that of the pad after the incidence of heavy wear. A  $100\text{-}\mu\text{m}$ - ( $4\times 10^{-3}$ -in.-) deep wear track was formed on this disk, which is extremely significant in view of the unmeasurably small disk wear observed after sliding against other carbon-graphite materials. Perhaps the use of graphite-cloth-reinforced composites in high-energy friction applications would benefit from the development of a specially formulated wear surface which would be integral with the reinforced substrate.

The wear of the boronated graphite material, against both the 17-22 AS steel and graphite-cloth-reinforced disk materials, was comparable to that of the CG-HB baseline material. This is somewhat unexpected in view of the low mechanical strength of the boronated graphite and the relatively high wear shown by the standard carbon graphite with  $\text{B}_4\text{C}$  additions (CG-BC). The extremely soft graphite must have effectively lubricated the sliding interface. There was no indication of abrasive disruption of the surface. The only surface features that can be related to wear are the presence of surface pits, as shown in figure 12.

In one instance, very severe wear to the boronated graphite pad was observed. This was a case in which the boronated graphite was subjected to sliding against a graphite-cloth-reinforced disk following heavy wear to the disk after sliding against GCRC pad material. The wear to the boronated graphite pads was clearly abrasive, and over half of the pad thickness was worn away before fracture occurred. This happened after about 5 seconds of sliding. One further test in which CG-HB was slid against the same graphite-cloth-reinforced composite disk showed similar results. Heavy abrasive wear to the CG-HB pad and disk was observed.

## CONCLUSIONS

Based on the results of friction and wear experiments on some carbon-graphite material systems, the following conclusions were drawn:

1. It was generally observed that smooth friction and low wear depended on main-

taining a continuous oriented graphitic shear layer on the sliding surface of the carbon-graphite pad.

2. The effect of binder level may be summarized as follows:

a. Decreasing the binder level from 70 parts to 60 parts per 100 parts filler resulted in increased wear, which correlated with a decrease in mechanical strength.

b. Further decreasing the binder level to 45 parts per 100 parts filler brought about a decrease in wear rate despite further strength reductions. This was related to the more graphitic structure of the low-binder-level formulation, with the associated improvements in graphite shear layer formation and oxidation resistance.

3. The addition of fine graphite fibers to the filler of the baseline carbon-graphite material resulted in a reduction in wear rate against both disk materials.

4. When boron carbide ( $B_4C$ ) was added to the baseline carbon-graphite formulation, a marked increase in wear rate was observed as a result of sliding against the 17-22 AS steel disk material.

5. The graphite-cloth-reinforced composite exhibited the lowest wear rate of all the carbon-graphite formulations against the 17-22 AS steel disk material. However, an unstable friction and wear transition was observed when sliding was against the graphite-cloth-reinforced composite disk material; heavy wear and erratic friction resulted.

6. The boronated graphite material, though much softer and weaker than the other experimental carbon graphites, showed wear rates and frictional behavior comparable to those of the baseline material.

Lewis Research Center,  
National Aeronautics and Space Administration,  
and  
U.S. Army Air Mobility R&D Laboratory,  
Cleveland, Ohio, March 19, 1975,  
505-04.

#### REFERENCES

1. Stanton, George E.: New Designs for Commercial Aircraft Wheels and Brakes. J. Aircraft, vol. 5, no. 1, Jan.-Feb. 1968, pp. 73-77.
2. Hooton, N. A.: Metal Ceramic Composites in High Energy Friction Applications. Bendix Technical J., vol. 2, Spring 1969, pp. 55-61.

3. Peterson, M. B.; and Ho, Ting-Long: Consideration of Materials for Aircraft Brakes. Rensselaer Polytechnic Inst., 1972; also NASA CR-121116, 1972.
4. Ho, Ting-Long; and Peterson, M. B.: Development of Aircraft Brake Materials - Evaluation of Metal and Ceramic Materials in Sliding Tests Simulation of Aircraft Braking. Rensselaer Polytechnic Inst., 1974; also NASA CR-134663, 1972.
5. Bill, Robert C.: Some Metal-Graphite and Metal-Ceramic Composites for Use as High Energy Brake Lining Materials. NASA TN D-7756, 1974.
6. Campbell, W. E.; and Kozak, Rose: Studies in Boundary Lubrication. III - The Wear of Carbon Brushes in Dry Atmospheres. ASME Trans., vol. 70, no. 5, July 1948, pp. 491-498.
7. Allen, Gordon P.; and Wisander, Donald W.: Oxidation Resistance of Selected Mechanical Carbons at 650<sup>0</sup> C in Dry Flowing Air. NASA TN D-7381, 1973.
8. Fechter, N. J.; and Petrunich, P. S.: Development of Seal Ring Carbon-Graphite Materials. (Tasks 8, 9, and 10). (Union Carbide Corp.; NAS3-13211.), NASA CR-121092, 1973.
9. Bisson, E. E.; Johnson, R. L.; and Anderson, W. J.: Friction and Lubrication Temperatures to 1000<sup>0</sup> F with Particular Reference to Graphite. ASME Paper 57-LUB-1, Oct. 1957.
10. Savage, Robert H.: Graphite Lubrication. J. Appl. Phys., vol. 19, no. 1, Jan. 1948, pp. 1-11.

TABLE I. - COMPOSITION, PROCESSING, AND PROPERTIES OF CARBON-GRAPHITE MATERIALS

[Binder material, no. 30 medium pitch, except for BG (no binder).]

	CG-HB (high binder)	CG-MB (medium binder)	CG-LB (low binder)	CG-FF (finely chopped fiber added)	CG-BC (B <sub>4</sub> C added)	GCRC (graphite- cloth reinforced composite)	BG (boronated graphite)
Filler material (graphite/ nongraphite), wt%	80/20	80/20	80/20	<sup>a</sup> 80/20	80/20	-----	100/0
Additive	-----	-----	-----	-----	B <sub>4</sub> C	-----	B <sub>4</sub> C
Binder level, pph	70	60	45	70	70	-----	7-10
Additive level, parts by weight <sup>b</sup>	-----	-----	-----	-----	5	-----	-----
Molding pressure, N/cm <sup>2</sup> (psi)	3465 (5000)	6929 (10 000)	13 858 (20 000)	3465 (5000)	3465 (5000)	-----	-----
Molding temperature, °C	100	100	100	100	100	-----	-----
Density, g/cm <sup>3</sup>	1.829	1.786	1.732	1.617	1.84	-----	1.65
Flexural strength, N/cm <sup>2</sup> (psi)	2630 (3810)	2310 (3350)	1260 (1830)	2020 (2930)	4430 (6430)	9600 (15 000)	~1400 (~2000)
Elastic modulus, MN/cm <sup>2</sup> (psi)	1.2 (1.7×10 <sup>6</sup> )	1.1 (1.6×10 <sup>6</sup> )	0.97 (1.41×10 <sup>6</sup> )	1.02 (1.48×10 <sup>6</sup> )	1.78 (2.58×10 <sup>6</sup> )	1.85 (2.7×10 <sup>6</sup> )	-----
Hardness, R <sub>S</sub>	106	98	84	76	96	-----	-----

<sup>a</sup>Graphite fibers.

<sup>b</sup>Per 100 parts of filler material.

TABLE II. - FRICTION AS FUNCTION OF LOAD FOR EXPERIMENTAL  
CARBON-GRAPHITE MATERIALS SLIDING AGAINST DISKS

(a) Disk material, 17-22 AS steel

Normal load		CG-HB	CG-MB	CG-LB	CG-FF	CG-BC	CGRC	BG
N	lbf	Friction coefficient						
187	42	0.14 .16	0.12	0.17	0.14	0.15	0.17	0.18
302	68	.15 .17	.16	.15	.15	.16	.22	.15
422	95	.14 .17	.16	.18	.16	.15	.30	.17
502	113	.20 <sup>a</sup> .18	<sup>a</sup> .15	.19	<sup>a</sup> .15	.18	.30	.20
543	122	<sup>a</sup> .20 .20	<sup>a</sup> .20	.20	<sup>a</sup> .16	.20	.29	.21

(b) Disk material, graphite-cloth-reinforced composite

187	42	0.17	0.17	0.20	0.18	0.17	0.21	0.24
302	68	.19	.15	.21	.24	.19	.22	.21
422	95	.20	.18	.18	.23	.20	.20	.20
502	113	.20	.20	.19	.23	.19	.19	.18
543	122	.21	.20	.20	.22	.19	.20	.18

<sup>a</sup>Sparks observed during sliding exposure.

TABLE III. - SPECIFIC WEAR RATES OF CARBON-GRAPHITE MATERIALS SLIDING AGAINST DISKS

(a) Disk material, 17-22 AS steel

Test type <sup>a</sup>	Frictional energy, kN-m	Specific wear rate, mm <sup>3</sup> /N-m	Test type <sup>a</sup>	Frictional energy, kN-m	Specific wear rate, mm <sup>3</sup> /N-m	Test type <sup>a</sup>	Frictional energy, kN-m	Specific wear rate, mm <sup>3</sup> /N-m
CG-HB			CG-FF			GCRC		
1	284	9.8×10 <sup>-6</sup>	1	295	4.2×10 <sup>-6</sup>	1	186	3.7×10 <sup>-6</sup>
2	148	<sup>b</sup> 400.0	3	940	4.0	2	450	3.4
1	260	8.2	2	262	<sup>b</sup> 28.0	3	350	7.9
2	283	7.9	3	294	19.0	Average wear rate <sup>c</sup>		4.9×10 <sup>-6</sup>
3	146	<sup>b</sup> 64.0	2	262	7.9	Standard deviation		1.8×10 <sup>-6</sup>
1	289	47.0	Average wear rate <sup>c</sup>		8.8×10 <sup>-6</sup>	BG		
Average wear rate <sup>c</sup>		18.0×10 <sup>-6</sup>	Standard deviation		6.1×10 <sup>-6</sup>	1	210	17.0×10 <sup>-6</sup>
Standard deviation		16.0×10 <sup>-6</sup>	CG-BC			2	290	4.3
CG-MB			1	169	140.0×10 <sup>-6</sup>	3	295	31.0
3	1560	24.0×10 <sup>-6</sup>	1	197	61.0	2	292	2.1
3	243	<sup>b</sup> 37.0	2	264	180.0	Average wear rate <sup>c</sup>		13.0×10 <sup>-6</sup>
1	191	230.0	3	313	14.0	Standard deviation		11.0×10 <sup>-6</sup>
1	176	95.0	1	203	29.0			
2	183	<sup>b</sup> 490.0	Average wear rate <sup>c</sup>		85.0×10 <sup>-6</sup>			
1	119	76.0	Standard deviation		64.0×10 <sup>-6</sup>			
Average wear rate <sup>c</sup>		110.0×10 <sup>-6</sup>						
Standard deviation		76.0×10 <sup>-6</sup>						
CG-LB								
2	300	19.0×10 <sup>-6</sup>						
3	357	6.4						
1	250	16.0						
1	267	6.3						
Average wear rate <sup>c</sup>		12.0×10 <sup>-6</sup>						
Standard deviation		5.7×10 <sup>-6</sup>						

<sup>a</sup>1 - a combination simulated-stop - constant-speed exposure.

2 - a load-variation test pattern exposure.

3 - a 422-N-normal-load, 26-m/sec exposure for 60 sec or longer.

<sup>b</sup>Spark generation occurred, with oxidation damage to the pad material.

<sup>c</sup>Not including tests during which spark generation occurred.

TABLE III. - Concluded.

(b) Disk material, graphite-fiber-reinforced composite

Test type <sup>a</sup>	Frictional energy, kN-m	Specific wear rate, mm <sup>3</sup> /N-m	Test type <sup>a</sup>	Frictional energy, kN-m	Specific wear rate, mm <sup>3</sup> /N-m
CG-HB			CG-BC		
1	324	3.4×10 <sup>-6</sup>	2	293	11.0×10 <sup>-6</sup>
2	302	7.3	GCRC		
CG-MB			1	259	<sup>d</sup> 17.0×10 <sup>-6</sup>
1	242	7.0×10 <sup>-6</sup>	2	354	4.0
2	305	44.0	BG		
CG-LB			1	242	12.0×10 <sup>-6</sup>
1	269	2.1×10 <sup>-6</sup>	2	253	6.7
2	286	10.0			
CG-FF					
1	288	2.1×10 <sup>-6</sup>			
2	394	3.1			

<sup>a</sup>1 - a combination simulated-stop - constant-speed exposure.

2 - a load-variation test pattern exposure.

<sup>d</sup>Severe wear to disk observed.

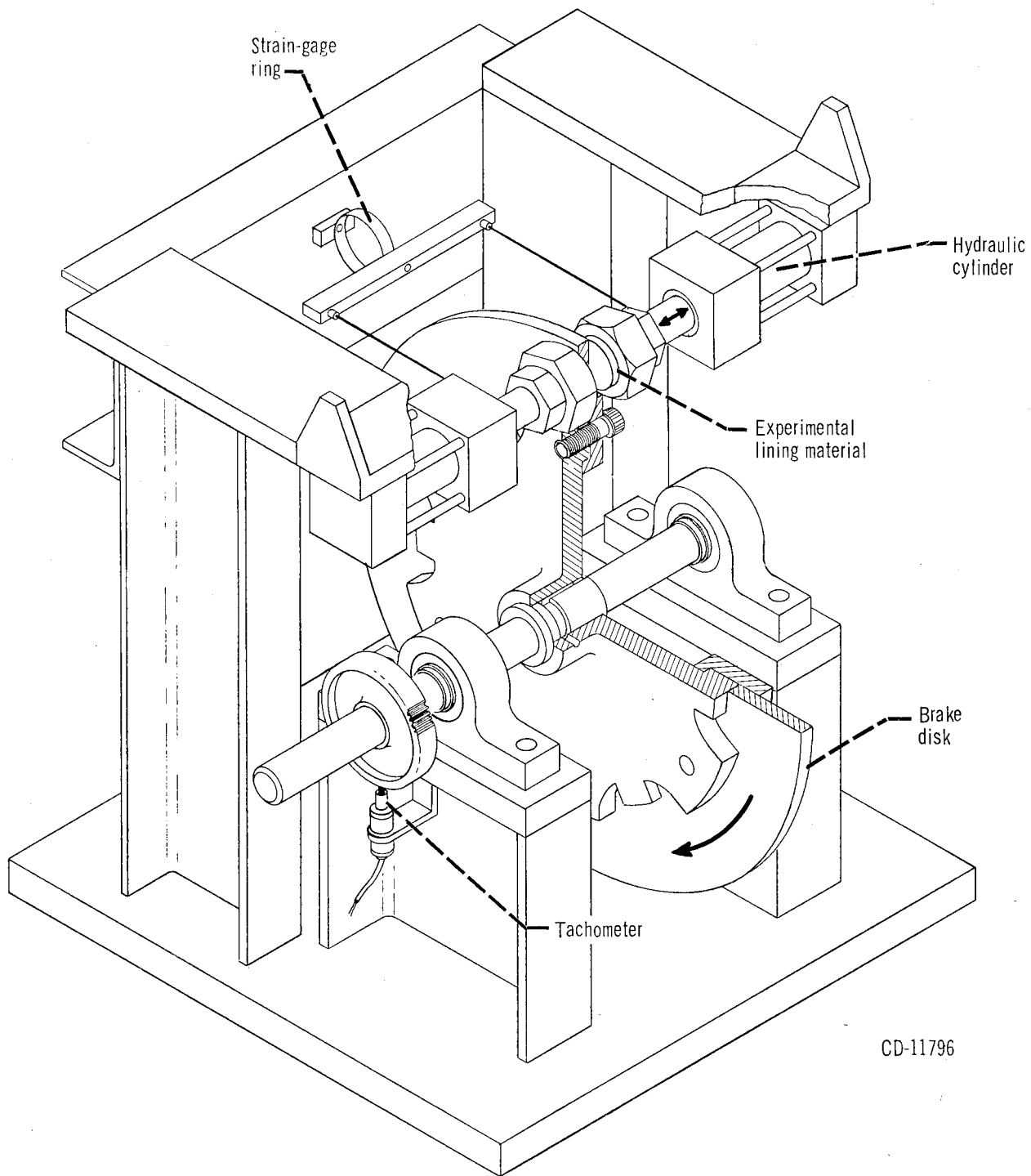


Figure 1. - Brake apparatus.

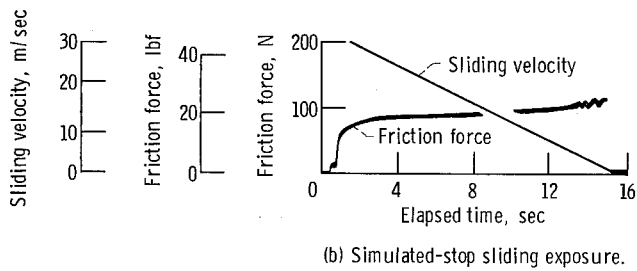
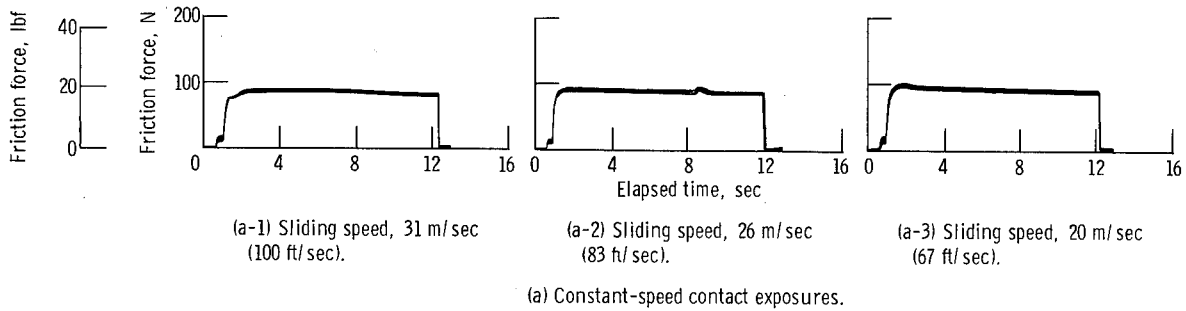


Figure 2. - Friction data obtained from carbon graphite - high binder (CG-HB) sliding against a 17-22 AS steel disk under a contact load of 382 N (86 lbf).

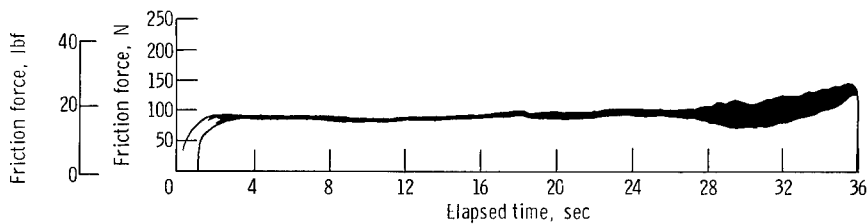
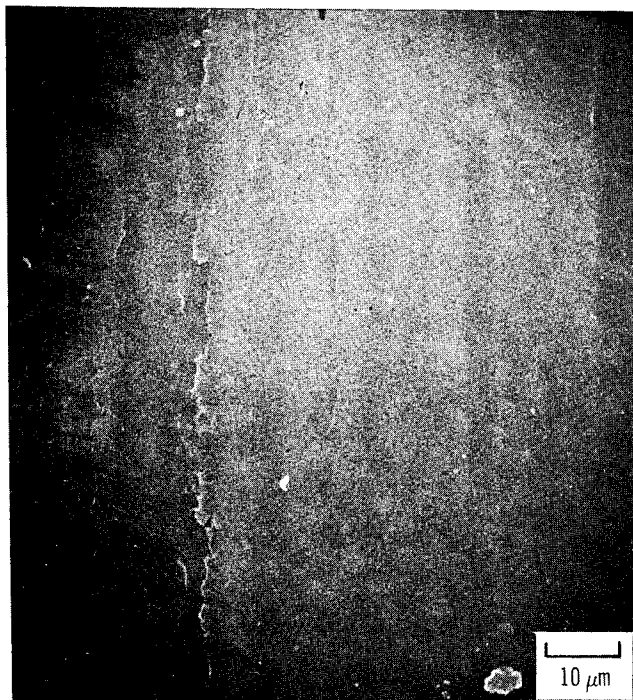


Figure 3. - Friction data obtained from carbon graphite - high binder (CG-HB) sliding against a 17-22 AS steel disk under prolonged, high-normal-load conditions. Contact time, 30 sec; contact load, 422 N (95 lbf); sliding velocity, 26 m/sec (83 ft/sec).

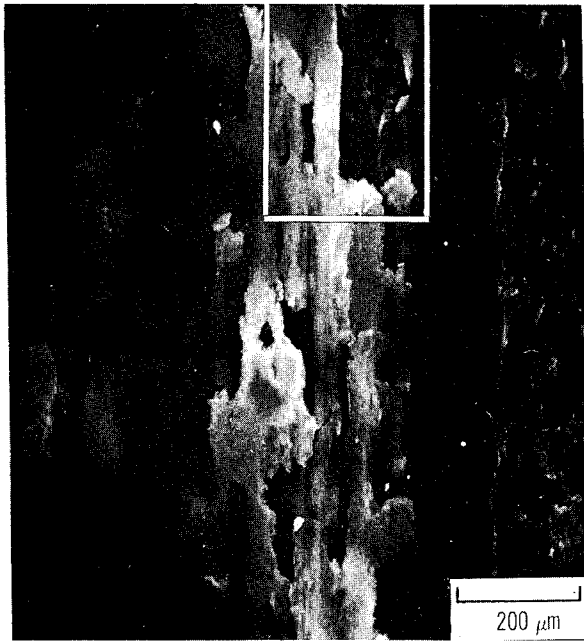


(a) Optical photograph.

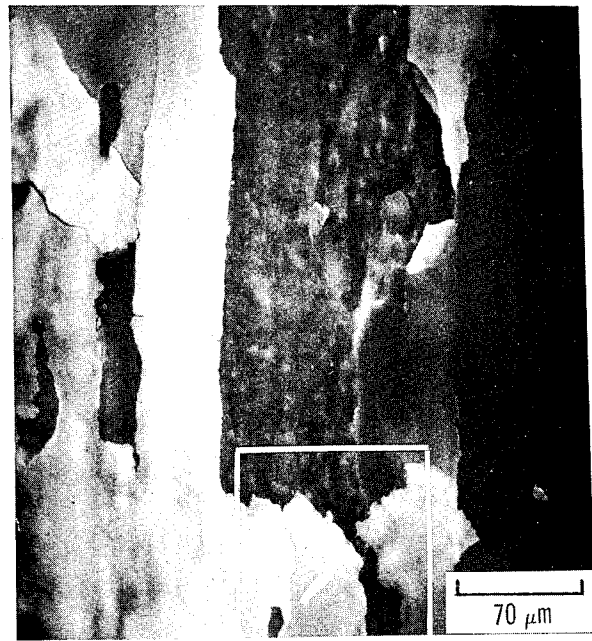


(b) Scanning electron micrograph.

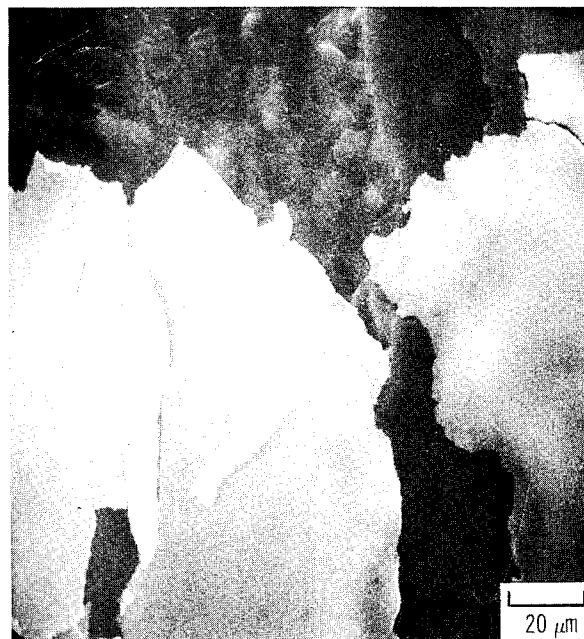
Figure 4. - Surface of carbon graphite – high binder (CG-HB) after a combination of simulated-stop and constant-speed exposures under a contact load of 382 N (86 lbf).



(a) Overview of blistered area.

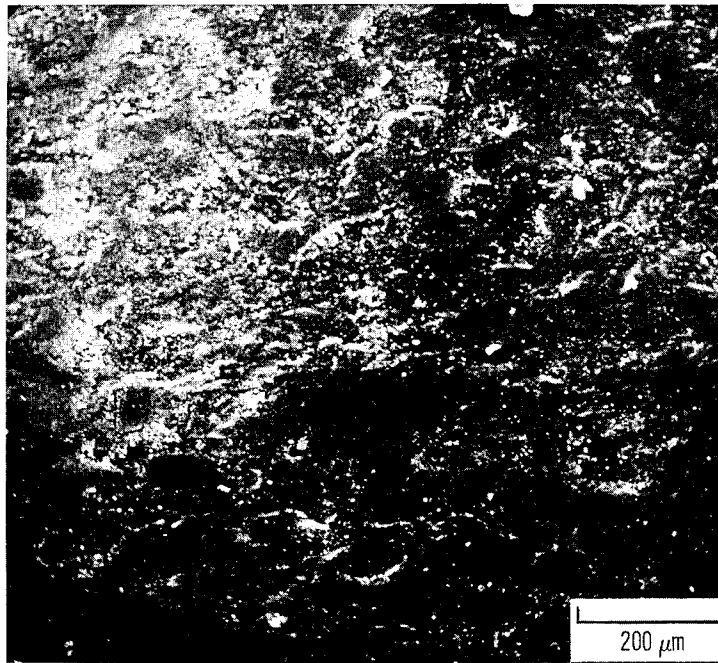


(b) Enclosed region in (a).

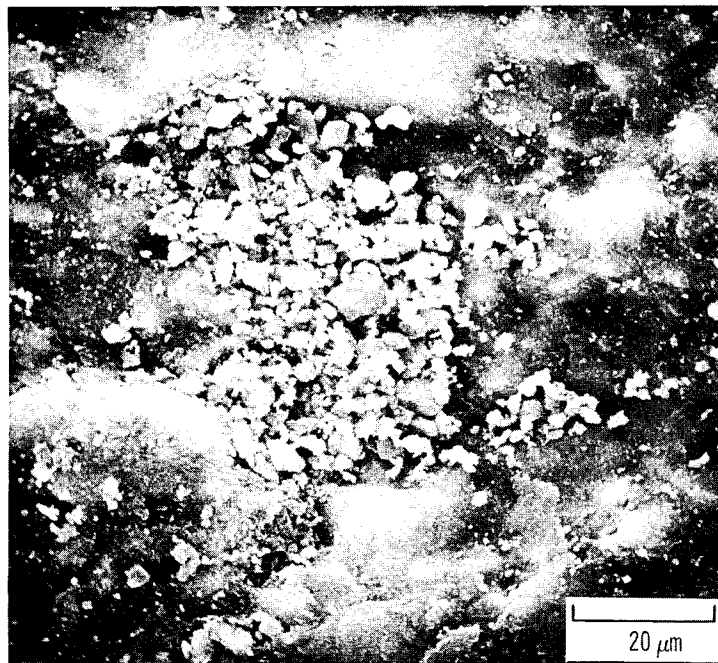


(c) Enclosed region in (b).

Figure 5. - Surface of carbon graphite – low binder (CG-LB) after 1 minute of sliding against a 17-22 AS steel disk at 26 m/sec (83 ft/sec) under a normal load of 422 N (95 lbf).

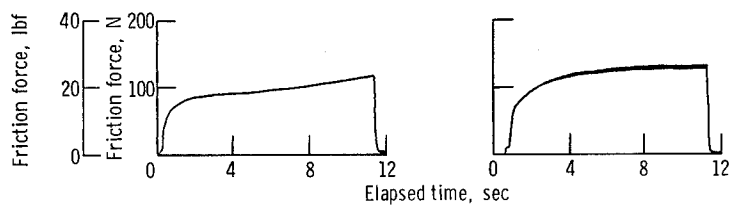


(a) Appearance of general surface.



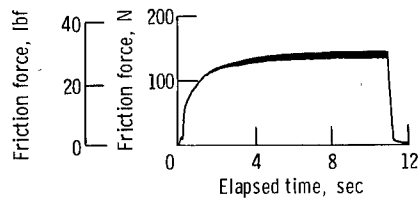
(b) Central portion of (a).

Figure 6. - Surface of carbon graphite - high binder (CG-HB) after sliding against a 17-22 AS steel disk in a load-variation-type test. Maximum normal load, 542 N (122 lbf); sliding speed, 26 m/sec (83 ft/sec).



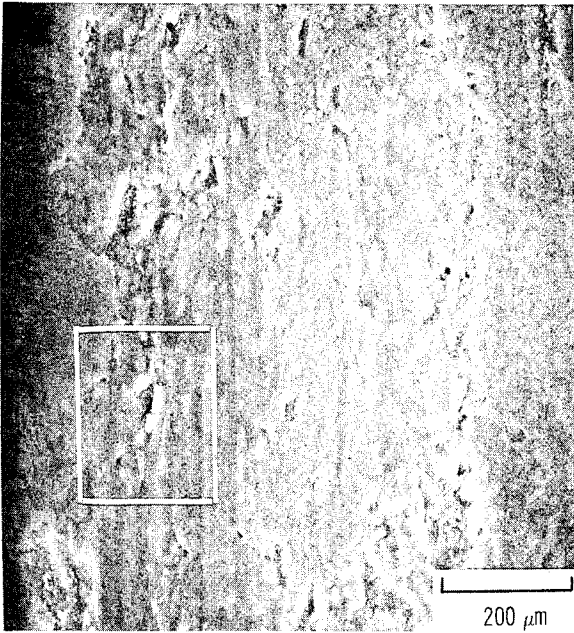
(a) Sliding speed, 31 m/sec (100 ft/sec).

(b) Sliding speed, 26 m/sec (83 ft/sec).

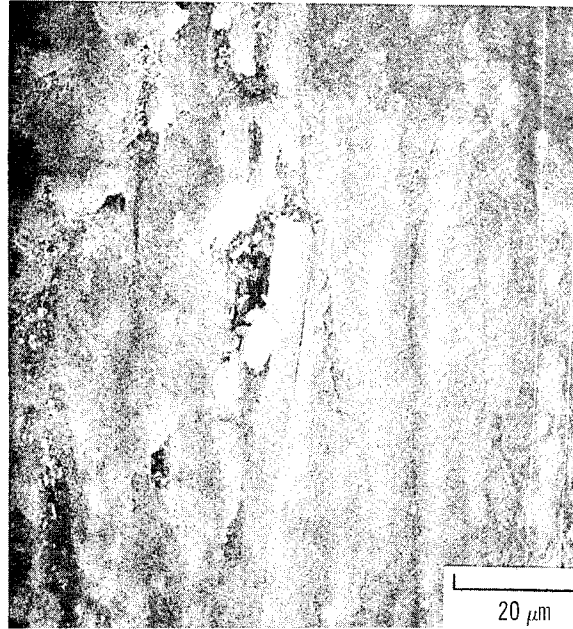


(c) Sliding speed, 20 m/sec (67 ft/sec).

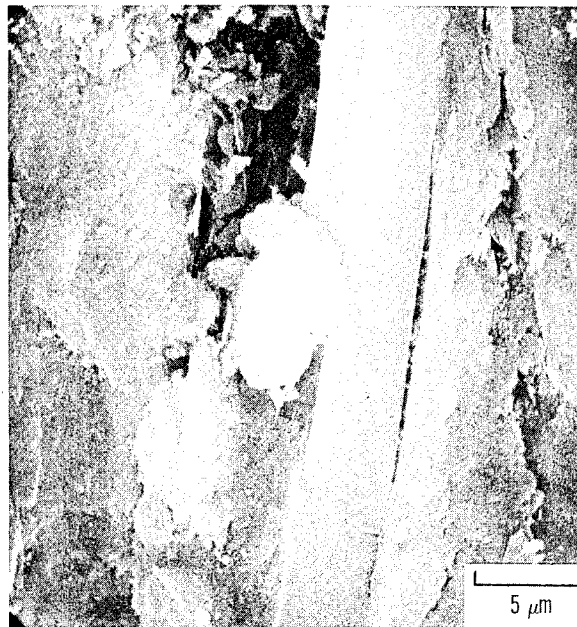
Figure 7. - Friction data obtained from carbon graphite - fine fibers (CG-FF) sliding against a 17-22 AS steel disk under a normal load of 382 N (86 lbf).



(a) Appearance of general surface.

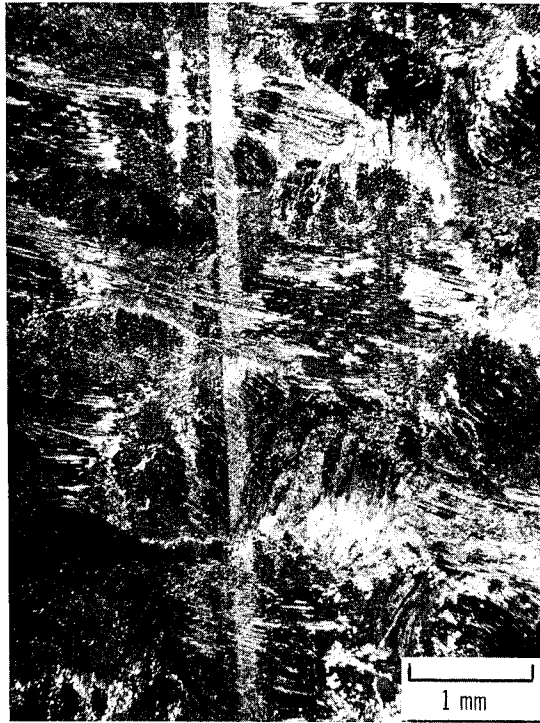


(b) Enclosed region in (a) showing fiber segment.

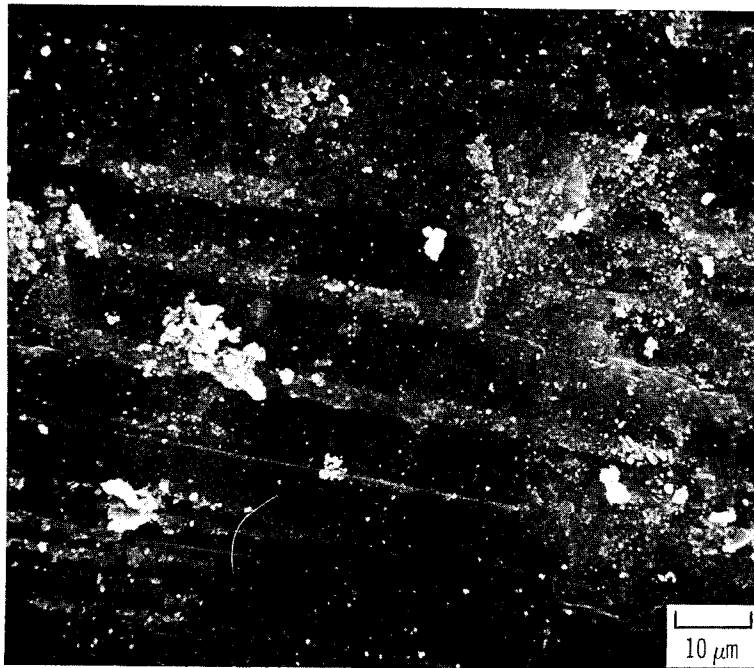


(c) Expanded view of fiber shown in (b).

Figure 8. - Surface of carbon graphite – fine fibers (CG-FF) after two 30-second sliding exposures against a 17-22 AS steel disk at 26 m/sec (83 ft/sec) under a normal load of 422 N (95 lbf).



(a) Optical photograph.



(b) Scanning electron micrograph.

Figure 9. - Surface of graphite-cloth-reinforced composite (GCRC) after sliding against a 17-22 AS steel disk in a simulated-stop – speed-variation test.

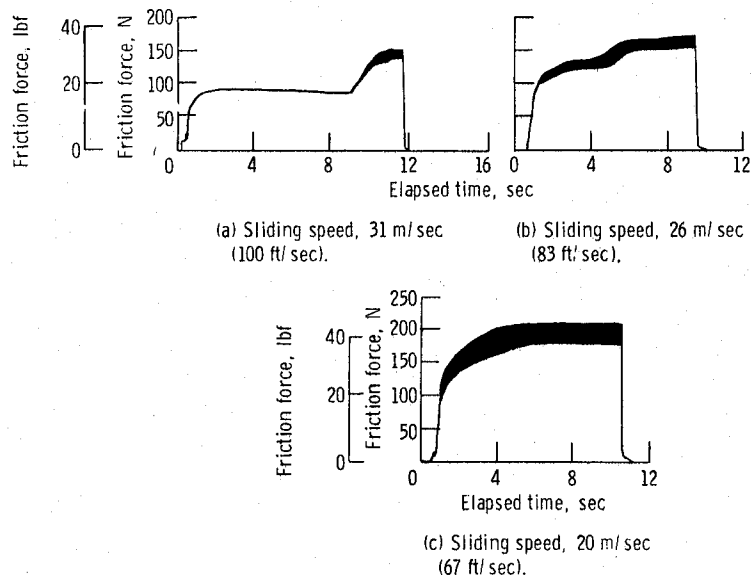


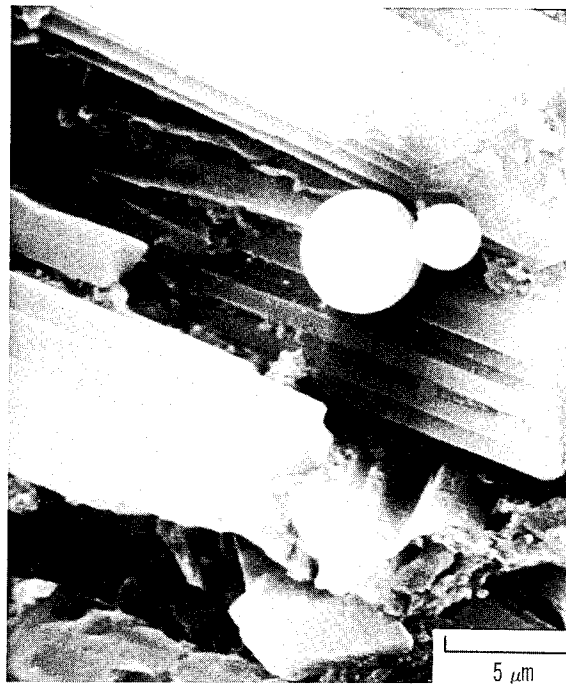
Figure 10. - Friction data obtained from graphite-cloth-reinforced composite (GCRC) sliding against a graphite-cloth-reinforced-composite disk under a normal load of 382 N (86 lbf).



(a) Area of exposed fiber structure.

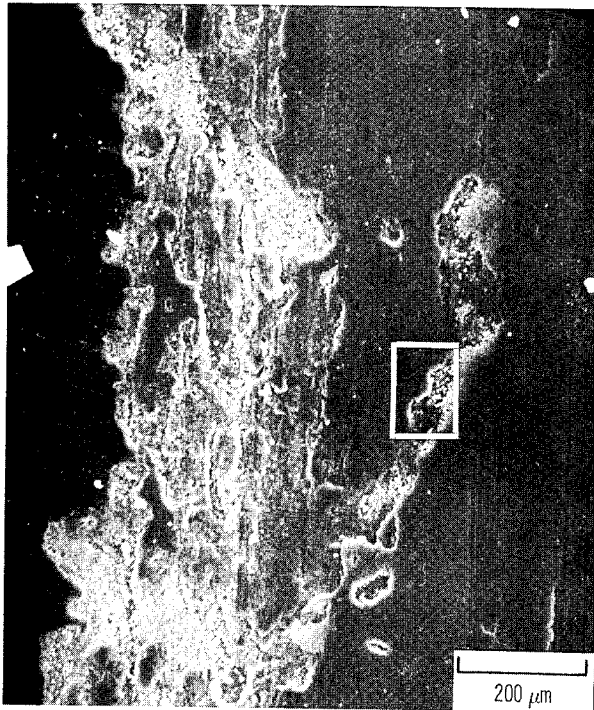


(b) Region in (a) showing fiber structure of reinforcing cloth.

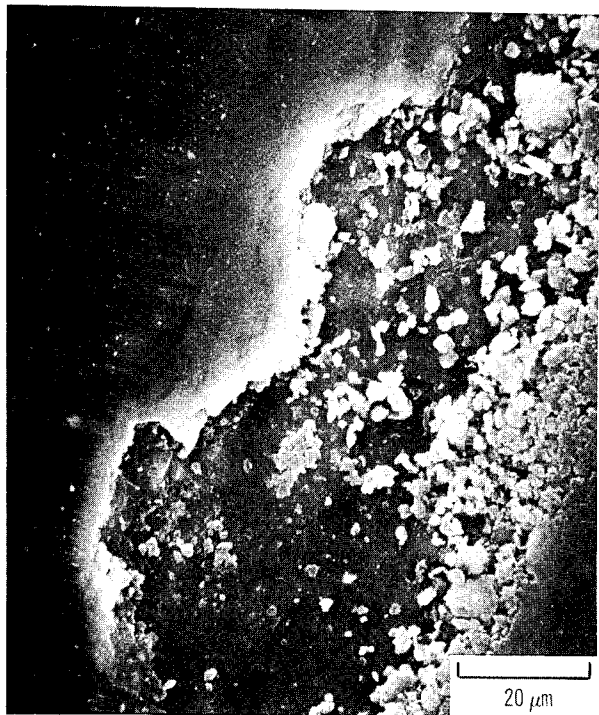


(c) Enclosed region in (a).

Figure 11. - Surface of graphite-cloth-reinforced composite (GCRC) after sliding against a graphite-cloth-reinforced disk in simulated-stop – speed-variation test shown in figure 10.



(a) General surface condition.



(b) Enclosed region in (a).

Figure 12. - Surface of boronated graphite (BG) after sliding against a graphite-cloth-reinforced composite disk in a simulated-stop - speed-variation test.